Estimating the maximum attachment performance of tree frogs on rough substrates

Julian K A Langowski[1)], Anne Rummenie[1)], Remco P M Pieters[1)], Alexander Kovalev[2)], Stanislav N Gorb[2)], Johan L van Leeuwen[1)]

[1)] Experimental Zoology Group, Wageningen University & Research, The Netherlands.

[2)] Functional Morphology and Biomechanics, Kiel University, Germany.

E-mail: julian.langowski@wur.nl

Abstract

Tree frogs can attach to smooth and rough substrates using their adhesive toe pads. We present the results of an experimental investigation of tree frog attachment to rough substrates, and of the role of mechanical interlocking between superficial toe pad structures and substrate asperities in the tree frog species *Litoria caerulea* and *Hyla cinerea*. Using a rotation platform setup, we quantified the adhesive and frictional attachment performance of whole frogs clinging to smooth, micro-, and macrorough substrates. The transparent substrates enabled quantification of the instantaneous contact area during detachment by using frustrated total internal reflection. A linear mixed-effects model shows that the adhesive performance of the pads does not differ significantly with roughness (for nominal roughness levels of 0–15 µm) in both species. This indicates that mechanical interlocking does not contribute to the attachment of whole animals. Our results show that the adhesion performance of tree frogs is higher than reported previously, emphasising the biomimetic potential of tree frog attachment. Overall, our findings contribute to a better understanding of the complex interplay of attachment mechanisms in the toe pads of tree frogs, which may promote future designs of tree-frog-inspired adhesives.

Keywords: Bioadhesion, biomimetics, bioinspired adhesive, *Litoria caerulea*, *Hyla cinerea*, surface roughness, mechanical interlocking.

1 Introduction

Strong, reversible, and repeatable attachment to a variety of substrates with different geometrical, mechanical, and chemical properties is a basic requirement both for climbing animals and for next-generation technological adhesives [1]. This overlap in functional demands has led to

a considerable transfer of knowledge between the fields of biological and technical adhesion (e.g. [2–7]), and to the design of a large number of biomimetic and bioinspired adhesives [3,8–10].

Geckos and tree frogs are the most prominent vertebrate models for the design of biomimetic adhesives [11–15]. The toes of geckos are ‘hairy’ structures covered by numerous microscopic setae ending in nanoscopic spatulae and can conform to minute asperities of the substrate, hence facilitating the generation of ‘dry’ intermolecular van der Waals (vdW) forces between toe and substrate [16–19]. The ventral epidermis on the toe pads of tree frogs is relatively smooth compared to that of the gecko, but it also forms a surface pattern consisting of microscopic prismatic cells that are covered with nanoscopic cellular protrusions (‘nanopillars’) and separated by channels [20,21]. In contrast to geckos, tree frogs rely on a wet environment, and their permeable skin is inherently moist [22–24]. Accordingly, their toe pads stand out as a model system for attachment in wet conditions. The toe pads have been proposed to give rise to ‘wet adhesion’ [25–30], which comprises capillary and hydrodynamic attachment forces ([31,32]; e.g. Stefan adhesion). VdW forces [25,33] and mechanical interlocking [25,34–36] have also been discussed to contribute to the adhesion (i.e. the attachment force normal to the substrate surface) and friction (i.e. the attachment force parallel to the substrate surface) of tree frogs.

Studying the fundamental mechanisms of tree frog attachment contributes not only to the understanding of the ecology [37,38] and evolution [39,40] of these animals, but also promotes the technical development of biomimetic adhesives for operation in a wet environment, for example in surgery [41] or robotics [42]. Measuring adhesion, friction, and the respective contact-area-normalised contact stresses as a function of substrate properties such as free surface energy, stiffness, or roughness is a common approach to elucidate the fundamental mechanisms of an attachment apparatus [43–46]. For example, insect claws can only interlock mechanically

54 with substrate asperities above a critical roughness [47,48]. Analogously, mechanical interlock-
55 ing of the superficial structures on a tree frogs' toe pad with substrate asperities should be—if
56 present at all—maximal when the nominal roughness R of the substrate (defined, unless men-
57 tioned otherwise, as the characteristic size of the substrate asperities) is similar or larger in size
58 than the pad surface structures (i.e. ≈ 300 nm for the nanopillars [21] and ≈ 10 µm for the epi-
59 dermal cells [20]). The attachment forces generated by the other proposed attachment mecha-
60 nisms might also be critically attenuated with increasing substrate roughness, for example by
61 reducing the effective contact area [49] or by meniscus cavitation [34,50].
62 Traditionally, the attachment performance of a whole tree frog is quantified by measuring
63 the angles at which a frog begins to slide on (sliding angle $\alpha_{\parallel}$) and finally falls off (falling angle
64 $\alpha_{\perp}$) from a substrate rotating around a horizontal axis (referred to as 'rotation platform';
65 [25,50,51]). These angles are proxies for the whole-animal (static) friction and adhesion, re-
66 spectively. Previous work shows slight variations of falling and sliding angle with increasing
67 roughness up to ca. 15 µm [34,43,50,52]. At higher roughness levels, adhesive [34,50] as well
68 as frictional [34] performance decline. For computation of the contact-area-normalised whole-
69 animal adhesion (i.e. tenacity), previous studies exclusively used the maximum total contact
70 area of all toe pads and neglected inertial loads acting on the pads. Measurements of the whole-
71 animal attachment performance on nano- to microrough substrates under control of substrate
72 surface energy, and under consideration of the instantaneous contact area (i.e. the actual contact
73 area just before falling) and of dynamic loads are largely missing, which may have led to an
74 underestimation of the attachment performance of tree frogs.
75 Here, we present a study of the whole-animal attachment performance of tree frogs as a
76 function of substrate roughness on smooth (i.e. a nominal roughness R = 0 µm), micro-
77 (R = 0.1 µm, 0.5 µm, 6 µm, and 15 µm), and macrorough (R = 200 µm) substrates in the spe-
78 cies *Litoria caerulea* and *Hyla cinerea*, which are among the most intensively studied tree frog

species [20,21,25,33,35,41,42,53,54]. Most previous studies included smooth and macrorough substrates, distinguishing these roughness levels as reference cases. Using a custom-built rotation platform, which allows the dynamic measurement of the instantaneous contact area, we aim to (i) characterise the whole-animal attachment performance on rough substrates, (ii) test whether mechanical interlocking contributes to the adhesion of the toe pads, and (iii) provide an estimate for the maximum adhesion performance of tree frogs' toe pads. As tree frogs frequently encounter substrates with very diverse properties [55], we expect that adhesion and friction are insensitive towards a large range of substrate roughness levels. If mechanical interlocking is present as proposed previously, we expect an increase in attachment performance with increasing roughness. In particular, the attachment performance should increase stepwise when the substrate roughness gets larger than the nanopillars (i.e. switching from 0.1 nm to 0.5 µm) or the epidermal cells (i.e. switching from 6 µm to 15 µm). A stepwise decrease in attachment performance may be expected at an even higher roughness (i.e. 200 µm), when the substrate asperities become too large to allow interlocking with the micro- to nanoscopic pad surface structures. As the animal-substrate contact area in friction measurements is dominated by the belly [28,29,52,56,57], we can only analyse the whole-animal performance with respect to friction.

2 Materials and methods

2.1 Ethical statement

All animals used in this study were bought from legal vendors. All procedures described were approved by the Animal Ethics Committee of Wageningen University & Research (WUR; permit number 2014126.d).

2.2 Experimental animals

Experiments were performed with adult individuals of *Litoria caerulea* (number $n = 6$, body mass $m = 46.8 \pm 13.4$ g, snout-vent-length $\ell_{SV} = 79.2 \pm 5.6$ mm; unless mentioned otherwise,

we report mean ± standard deviation throughout this study) and *Hyla cinerea* ($n = 6$, $m = 8.7 \pm 1.7$ g, $\ell_{SV} = 48.7 \pm 1.6$ mm). The animals were housed, separated by species, in $0.6 \cdot 0.6 \cdot 1.2$ m^3 (width · length · height) large terraria, with six frogs per terrarium, at the CA-RUS research facility at WUR. The terraria were enriched with plants (*Ficus spec.*) and scaffolds of polypropylene-pipes. Temperature and relative air humidity were kept at 24–26 °C and 45–85%, using heating mats and a semi-automatised sprinkler system spraying demineralised water (Bitter Watertreatment, Netherlands), respectively. The frogs were kept at a 12 h : 12 h dark-light-cycle and fed 2–3 times per week with 3–5 live crickets enriched with vitamin/mineral powder (Dendrocare, AmVirep, Netherlands) per individual; water was supplied *ad libitum*. The room air was filtered for pathogens with an air purifier (WINIX U300, Winix, USA). The frogs were monitored daily for their wellbeing.

2.3 Test substrates

Transparent, stiff substrates with a defined roughness and a surface area of $290 \cdot 210$ mm^2 were produced in a two-stage-casting-process (similar to [58,59]). To create substrates with nominal roughness levels of 0 µm (smooth), 0.1 µm, 0.5 µm, 6 µm, 15 µm, and 200 µm (macrorough), a thin sheet of plexiglas, diamond lapping film (661X, 3M, USA), or conventional sandpaper (grit size 80, KWB, Germany) with the according particle size was glued into an aluminium mould (Figure 1A). Polydimethylsiloxane (PDMS; Sylgard 184, Dow Corning, USA) was prepared at a base:curing-agent ratio of 10:1, degassed in a vacuum-oven, and filled into the mould to create a negative of the rough surface (Figure 1B). Before casting, the mould was slightly tilted to avoid bubble formation. After curing, the PDMS-negative was removed (Figure 1C) and filled with vacuum-degassed epoxy resin prepared at a base:curing-agent ratio of 1:0.9 (Crystal Clear 200, Smooth-On, USA; Shore hardness = 80 D, Elastic modulus ≈ 400 MPa; Figure 1D), which resulted in a positive cast of the rough surface (Figure 1E).

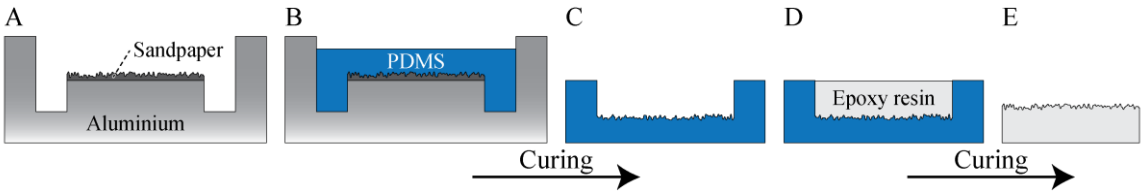

Figure 1. Generation of the transparent and stiff test substrates with defined roughness.

Surface roughness was characterised and spatial homogeneity of the surface profiles of the test substrates was ensured using a VR-3100 3D measuring macroscope (Keyence, Japan) and a New View 6000 white light interferometer (Zygo, USA). Conventional roughness parameters of the substrates are shown in Table 1, a more elaborate roughness analysis can be found in section SI.2.1. With an OCAH 200 contact angle measuring system (DataPhysics Instruments, Germany) and the sessile drop method, we computed for the hydrophilic substrate material (water contact angle 71.92 ± 2.07°) a free surface energy γ of 39.2 mJ m^{-2} (dispersive component γ_d = 30 mJ m^{-2}, polar component γ_p = 9.2 mJ m^{-2}) with the Owens, Wendt, Rabel, and Kaelble (OWRK) method ([60–62]; see section SI.2.2).

Table 1. Conventional roughness parameters R_a (arithmetic average roughness) and *RMS* (root mean squared roughness) of the used substrates in µm (mean ± standard deviation, n = 10). For the smooth to 15 µm substrates, roughness was measured by white light interferometry, for the macrorough substrate with profilometry (120× magnification).

	Magnification	Smooth	0.1 µm	0.5 µm	6 µm	15 µm	Macrorough
R_a	5×	0.024±0.007	0.438±0.022	0.476±0.017	0.405±0.025	0.441±0.046	88.214±11.893
	50×	0.005±0.002	0.425±0.023	0.474±0.032	0.410±0.072	0.484±0.122	
RMS	5×	0.053±0.014	0.591±0.030	0.628±0.055	0.684±0.029	0.965±0.076	N/A
	50×	0.006±0.002	0.534±0.028	0.579±0.034	0.667±0.096	0.961±0.141	

2.4 Experimental setup and protocol

A custom-built rotation platform was used to quantify the whole-animal attachment performance of the studied frog species (Figure 2A). The test substrates were rotated around a horizontal axis at an angular speed of ca. 3.6° s^{-1}, driven by a RS Pro brushed DC geared motor (RS Components, Netherlands) via a pulley-timing-belt-system (27-T5; Mädler, Germany). A custom-programmed Arduino (Arduino Uno revision 3, Arduino) read out the platform angle from an angle sensor (981 HE special, Vishay Spectrol, USA; linearity ± 0.5%).

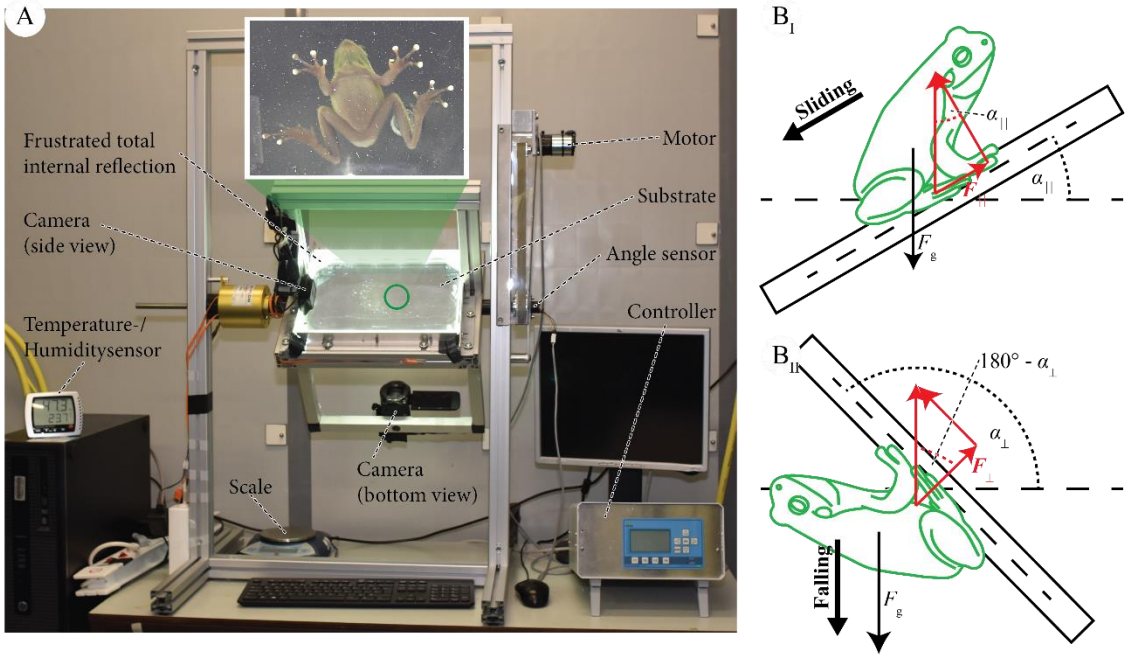

Figure 2. (A) Rotation platform setup (inset: example of the recorded bottom view of a frog clinging to the rotating substrate). Free body diagrams of a frog at the onset of (B_I) sliding and (B_{II}) falling. $\alpha_\perp$ falling angle, $\alpha_\parallel$ sliding angle, F_g body weight, $F_\perp$ adhesion, $F_\parallel$ friction.

Four LED-strips (LS-OO06-STWH-SD111; Intelligent LED Solutions, UK) were attached to the sides of the transparent substrate such that the emitted light was reflected internally. This allowed us to visualise the instantaneous pad-substrate contact area by frustrated total internal reflection (FTIR; [63]), which utilises the frustration of the internal reflection at locations of animal-substrate contact, causing local light scattering (inset in Figure 2A). The contact area was recorded ventrally with a HC-VX980 camcorder rotating with the substrate (Panasonic, Japan; 3840 · 2160 pixels, effective pixel size ≈ 90 · 90 µm^2) at 30 frames per second, resulting in an angular step size of 0.12° per frame. The video recordings and angle measurements were synchronised using a sound signal (duration < 5 ms) at regular time intervals ($\Delta t \approx 2.14$ s). The animals were filmed laterally with a C930e webcam (Logitech, Switzerland; 1920 · 1080 pixels, 30 frames per second) to inspect general body positing and movements.

Prior to each trial, the animals were rinsed carefully with demineralised water to remove contaminations that could influence attachment performance, and subsequently put on a smooth

polymer sheet to standardise the amount of liquid covering the ventral body surface. Six individuals each of *L. caerulea* and *H. cinerea* were tested for the six substrates with different roughness levels in a randomised order. To compensate for the variation in the measurements due to behavioural variation in the animals, we repeated each individual-roughness-combination 10 times (i.e. a trial), leading to a total of 720 trials (60 per species and roughness). In each trial, individual animals were placed head upwards on the substrate and rotated from a horizontal (0°) into a vertical (90°) and finally an overhanging position (> 90°). Belly-substrate contact was impaired by gently prodding the animals with a soft object. Trials were excluded when the frogs jumped off the substrate, moved outside the substrate area with specified roughness, or made extensive contact with body parts other than the toe pads before falling (in adhesion measurements), leading to 133 and 72 trials of *L. caerulea*, and 106 and 70 trials of *H. cinerea* for further analysis of their adhesion and friction performance, respectively. These trials include cases with only a few toes in contact.

2.5 Data analysis and statistics

Data analysis was performed with a custom-made MATLAB routine (Version R2015a, The Mathworks, USA). From the videos, the angles at which the frogs started sliding ($\alpha_{||}$) and lost contact to the substrate ($\alpha_{\perp}$) with all four limbs were identified. For the determination of the instantaneous contact area A just before falling, we measured the contact area of all toes in contact at the last recorded moment before detachment, at which the number of toes in contact was constant and the contact area of individual toes was not yet decreasing (i.e. static contact; see also Figure SI.6). The instantaneous contact area was quantified with ImageJ (Version 1.51g, National Institutes of Health, USA). This was not possible for the macrorough substrate because of too strong scattering of the totally internally reflected light.

Before each trial, snout-vent-length ℓ_{SV} was recorded by a calibrated dorsal photograph made with a Nikon 5500 camera using a Nikon AF-NIKKOR 24 mm f/2.8 D lens

(6000 · 4000 pixels, effective pixel size 47 · 47 µm^2); immediately after each trial, body mass *m*, environmental temperature *T*, and relative air humidity *H* were recorded using an OHAUS Scout Pro balance (Parsippany, USA; resolution: 0.01 g) and a testo 608-H1 hygrometer (Testo Ltd, UK; resolution: 0.1 °C, 0.1%), respectively.

From the sliding and falling angle ($\alpha_\parallel$ and $\alpha_\perp$), body mass *m*, and instantaneous contact area *A*, we computed adhesion $F_\perp$, static friction $F_\parallel$, and the adhesive contact stress (i.e. tenacity $\sigma_\perp$) as follows (Figure 2B, [51]):

$$F_\perp = mg\cos(180 - \alpha_\perp) = -mg\cos\alpha_\perp \qquad 90° < \alpha_\perp < 180° \qquad (1)$$

$$F_\parallel = mg\sin\alpha_\parallel \qquad 0° < \alpha_\parallel < 90° \qquad (2)$$

$$\sigma_\perp = \frac{F_\perp}{A} \qquad (3)$$

In these equations, we assume an equal distribution of load over all limbs and toes, and neglect inertial effects. The potential effects of substrate roughness on the attachment performance of tree frogs were analysed by fitting the falling angle $\alpha_\perp$ and sliding angle $\alpha_\parallel$ as a function of substrate, species, and body mass in a linear mixed-effect model in MATLAB (significance level α = 0.05). Based on the Akaike information criterion adjusted for small sample sizes (AICc; [64]), snout-vent-length, temperature, and relative humidity were excluded as fixed effects. Individual identity was fitted as random intercept to correct for interindividual variation that is not accounted by the fixed effects. Measurement date was fitted as additional random intercept to correct for variation between measurement days. Moreover, the interaction between individual identity and substrate, as well as between individual identity and repetition number were fitted as random intercepts to correct for pseudo-replication and to quantify the variation of an individual within a given substrate and repetition number, respectively. For the model diagnostics see section SI.4.

3 Results

Tree frogs are able to generate adhesion and friction on substrates with different roughness levels. Over the course of measurements, temperature and relative air humidity were 23.3–26.3 °C and 39.8–69.0%, respectively. During single trials, the animals regularly moved across the rotating platform, requiring prodding with the hands of the experimenter to keep the frogs on the platform (Figure 3). Typical changes in body posture were observed, with frogs taking a splayed body posture with increasing substrate inclination, as discussed in detail elsewhere [52,65]. Over the course of one trial, large changes in the number of contact points and in the size of the instantaneous contact area were observed, ranging from—in addition to the toes—full belly contact to the contact of only a few toes of two limbs (Figure 3).

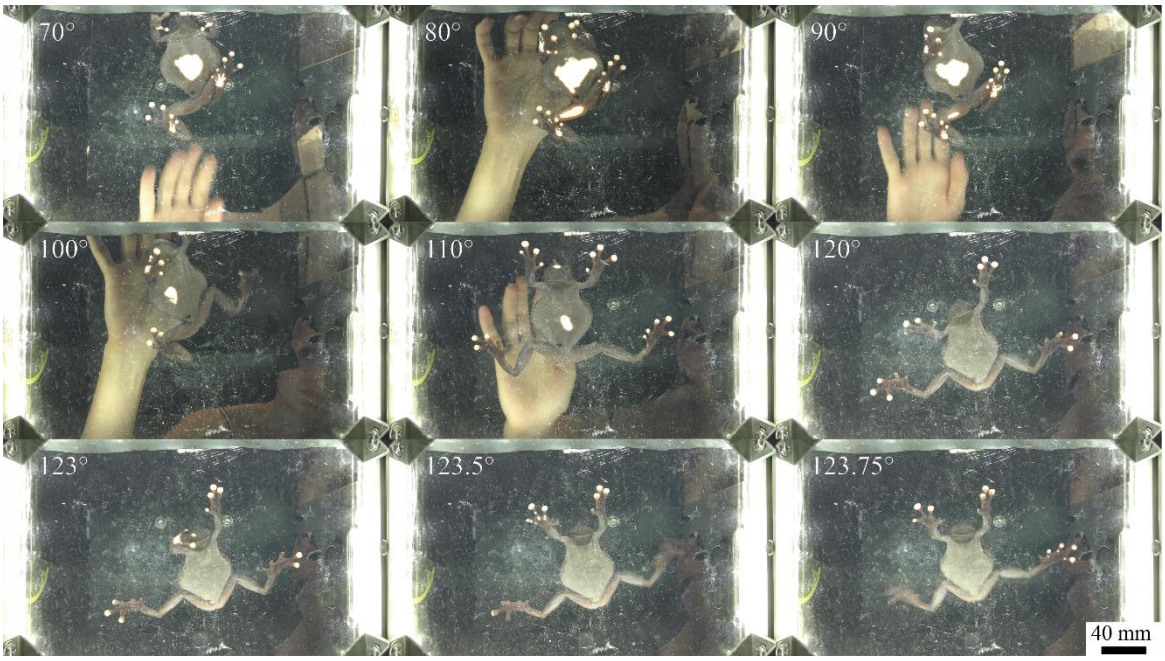

Figure 3. Rotation platform trial for an individual of *L. caerulea* on a smooth substrate. At platform angles ≤ 100°, the belly contributes to the overall contact area. Just before detachment (angles ≥ 123°), quick limb movements are visible, which result in time and space dependent variations of the ensemble of pad-substrate contact areas.

Interestingly, we observed several instances where frogs clinging to the substrate at an angle of approximately 120–130° were able to remain attached although temporarily the fore-limbs completely detached from the substrate and the animals swung back- and forwards (Figure 4).

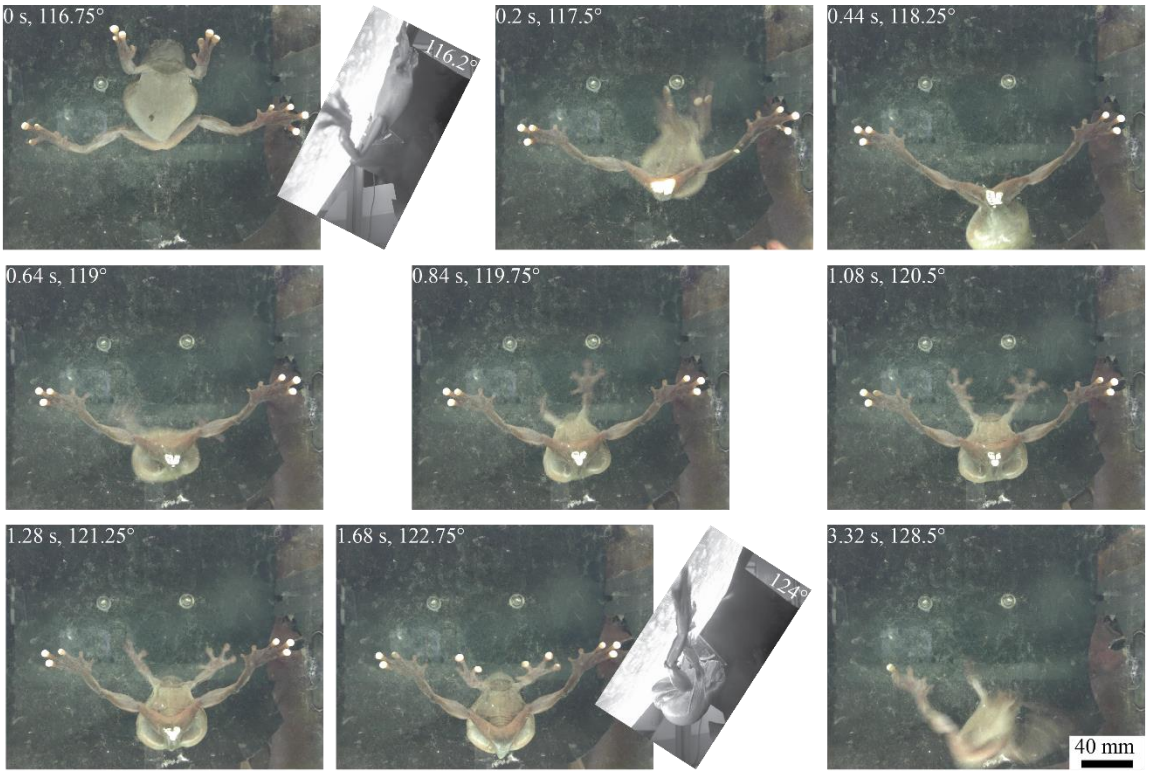

Figure 4. Attachment dynamics of *L. caerulea* clinging to a rotating, overhanging, smooth substrate. After detachment of the forelimbs, the body swings backwards by more than 90°. During the swinging phase, inertial loads are likely to act on the attachment interface in addition to the static body weight. Insets show the body posture in lateral view. To improve clarity, the images were filtered by outlier-removal (ImageJ).

In the following sections, we describe the adhesion performance of the toe pads and the friction performance of whole animals for the studied frog species.

3.1 Adhesion performance

For *L. caerulea*, the falling angle $\alpha_{\perp}$ ranges from 93.0 ± 13.4° (macrorough substrate) to 129.1 ± 11.2° (0.1 µm substrate; Figure 5). The falling angles on the 0.1 µm, 0.5 µm (118.1 ± 24.4°), 6 µm (128.2 ± 12.6°), and the 15 µm substrate (128.8 ± 14.7°) do not differ significantly from $\alpha_{\perp}$ on the smooth substrate (119.4 ± 18.2°), whereas falling angles on the macrorough substrate are significantly lower by 36.1 ± 4.9° than on the smooth substrate (estimate ± 95% confidence interval [*CI*]; see Table 2 for the linear mixed-effect model statistics). The falling angle scales negatively with body mass m (slope = −0.34 ± 0.28° g^{-1}, estimate ± 95% *CI*; $t = -2.337$, $DF = 231$, $p = 0.020$).

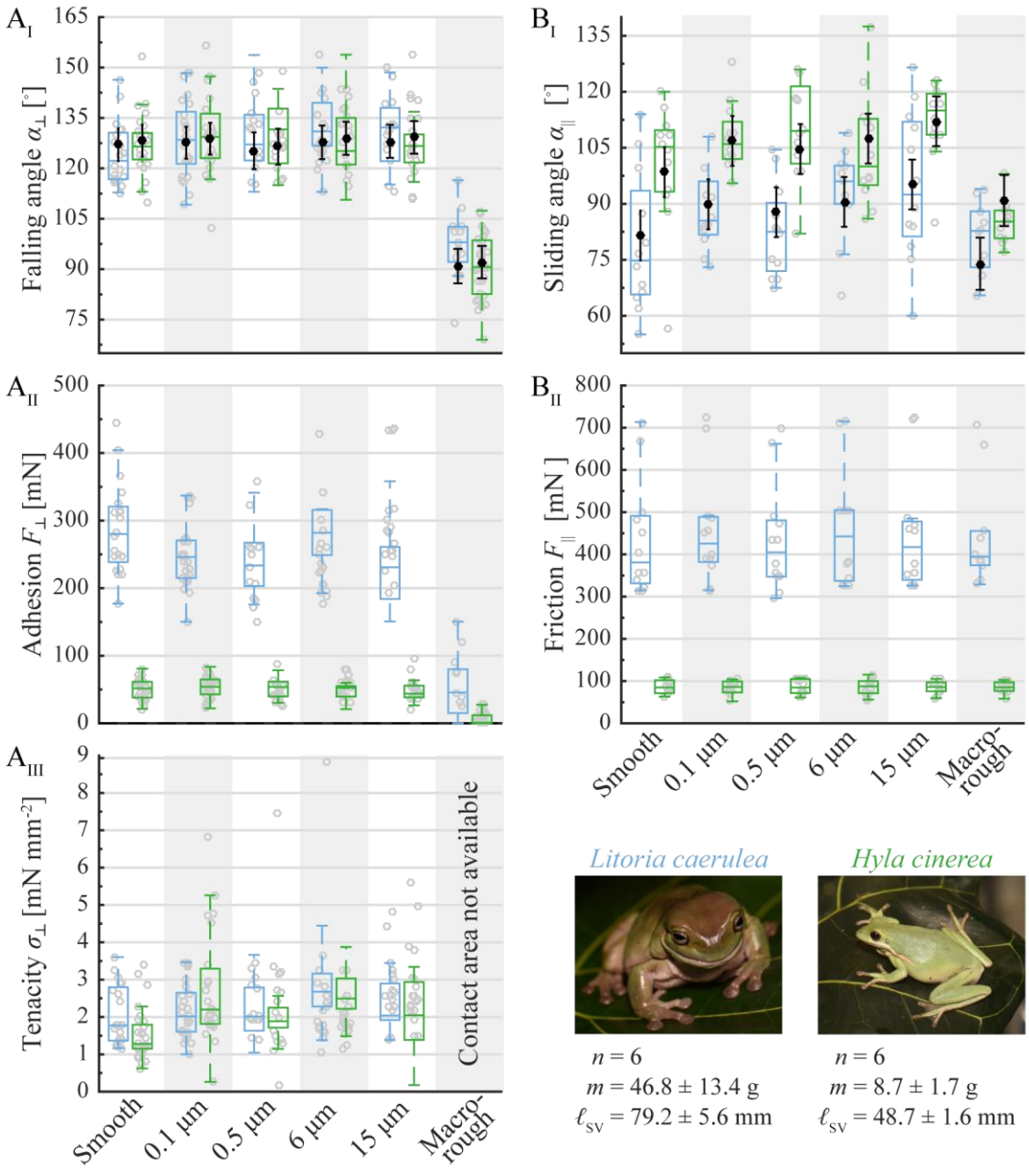

Figure 5. (A_I) Falling angle $\alpha_\perp$, (A_{II}) adhesion $F_\perp$, and (A_{III}) tenacity $\sigma_\perp$, as well as (B_I) sliding angle $\alpha_\parallel$ and (B_{II}) (static) friction $F_\parallel$ as a function of (nominal) substrate roughness R for *Litoria caerulea* (blue) and *Hyla cinerea* (green). For sliding angles $\alpha_\parallel > 90°$, the friction $F_\parallel$ was computed with $\alpha_\parallel = 90°$. Boxes indicate median, and 25th and 75th percentiles of the measured values. Values that are a located more than 1.5 times the interquartile range above or below the boxes are shown as outliers. For the falling and sliding angle, black dots and whiskers denote the mean values and the 95% confidence intervals predicted from the linear mixed-effects models. Strong scattering of the internally reflected light prevented the measurement of the contact area and thus of the tenacity on the macrorough substrate.

The adhesion $F_\perp$ of *L. caerulea* ranges between 192.8 ± 85.7 mN and 282.1 ± 88.5 mN for roughness levels between smooth and 15 µm. On the macrorough substrate, $F_\perp$ drops by 81% to 50.2 ± 63.5 mN, if compared to the smooth substrate; adhesion on the macrorough substrate is significantly different from the other roughness levels according to one-way ANOVA with

Bonferroni correction ($F[5,100] = 29.98$, $p < 0.001$). The adhesive tenacity $\sigma_{\perp}$ ranges from 2.1 ± 0.8 mN mm^{-2} (smooth substrate) to 2.8 ± 0.9 mN mm^{-2} (15 µm substrate). The tenacity measures are not significantly different, as determined by one-way ANOVA with Bonferroni correction ($F[4,88] = 1.46$, $p = 0.220$). Tenacity could not be quantified for the macrorough substrate because of too strong scattering of the internally reflected light. Peak tenacities of 8.8 mN mm^{-2} were measured.

Table 2. Fixed-effects coefficient estimates of the linear mixed-effects model for the falling angles of tree frogs on substrates with different roughnesses. *SE* standard error, *DF* degrees of freedom, *t* t-statistic, *p* p-value.

	Estimate	***SE***	***DF***	***t***	***p***
Intercept[a]	142.73	7.26	231	19.665	<0.001
Hyla cinerea	−11.60	6.07	231	−1.912	0.057
0.1 µm	0.60	2.36	231	0.254	0.799
0.5 µm	−1.78	2.69	231	0.287	0.774
6 µm	0.71	2.48	231	0.419	0.676
15 µm	1.02	2.42	231	−0.661	0.510
Macrorough	−36.12	2.47	231	−14.619	<.001
Body mass	−0.34	0.14	231	−2.337	0.020

[a] i.e. *Litoria caerulea* on the smooth substrate.

Similar trends were observed for the adhesion performance of *H. cinerea*, and the linear mixed-effects model does not show significant differences between the two species ($t = -1.912$, $DF = 231$, $p = 0.057$). Falling angles range from $126.9 \pm 8.2°$ to $130.1 \pm 9.2°$ for roughness levels between smooth and 15 µm, and the falling angle decreases significantly on the macrorough substrate, if compared to the other roughness levels. Compared to *L. caerulea*, *H. cinerea* generates much lower adhesion of 46.9 ± 15.1 mN to 54.5 ± 16.0 mN for roughness levels between smooth and 15 µm. On the macrorough substrate, *H. cinerea* barely adheres ($F_{\perp} = 2.0 \pm 14.2$ mN). The tenacity varies between 1.5 ± 0.7 mN mm^{-2} and 2.8 ± 1.1 mN mm^{-2} on the five less rough substrates, mostly without significant differences; only on the 0.1 µm ($p = 0.003$) and the 15 µm ($p = 0.003$) substrate, the frogs generated significantly higher tenacities compared to the smooth substrate, as found in a multiple comparison using Bonferroni correction.

3.2 Friction performance

The sliding angle $\alpha_{||}$ of *L. caerulea* ranges between 79.4 ± 18.6° (smooth) and 81.1 ± 9.5° (macrorough). Compared to the smooth substrate, $\alpha_{||}$ is significantly higher by 8.4–13.6° (estimates) on the 0.1 µm, the 6 µm, and the 15 µm substrate (Table 3). For the macrorough substrate, lower sliding angles were measured than on the smooth substrate (difference = −7.6 ± 8.5°, estimate ± 95% *CI*), but this difference is just not statistically significant ($p = 0.081$). In contrast to the falling angle, the scaling of sliding angle with body mass m is not significant (slope = −0.14 ± 0.29° g^{-1}; $t = -0.923$, $DF = 134$, $p = 0.358$).

Table 3. Fixed-effects coefficient estimates of the linear mixed-effects model for the sliding angles of tree frogs on substrates with different roughnesses. Symbols as in Table 2.

	Estimate	***SE***	***DF***	***t***	***p***
Intercept[a]	87.94	7.75	134	11.352	<0.001
Hyla cinerea	11.73	6.33	134	1.855	0.066
0.1 µm	8.35	4.21	134	1.984	0.049
0.5 µm	6.22	4.21	134	1.478	0.142
6 µm	8.98	4.21	134	2.135	0.035
15 µm	13.64	4.21	134	3.242	0.002
Macrorough	-7.58	4.31	134	−1.760	0.081
Body mass	-0.14	0.15	134	−0.923	0.358

[a] i.e. *Litoria caerulea* on the smooth substrate

The maximum friction force $F_{||}$ generated by *L. caerulea* ranges between 435.4 ± 135.3 mN (smooth) and 458.0 ± 131.6 mN (0.1 µm). Differences between the roughness levels are not significant, as determined by one-way ANOVA with Bonferroni correction ($F[5,64] = 0.08$, $p = 0.995$).

H. cinerea shows sliding angles $\alpha_{||}$ between 85.2 ± 5.6° (macrorough) and 112.3 ± 10.5° (15 µm). The sliding angle was not significantly different between *L. caerulea* and *H. cinerea* ($t = 1.855$, $DF = 134$, $p = 0.066$). The friction $F_{||}$ of *H. cinerea* ranges between 83.4 ± 18.4 mN (0.1 µm) and 86.3 ± 18.5 mN (0.5 µm). An one-way ANOVA with Bonferroni correction does not show significant differences in the friction generated on the different substrates ($F[5,66] = 0.05$, $p = 0.998$).

4 Discussion

4.1 Effects of substrate roughness on attachment performance

Figure 6 provides an overview of the effect of substrate roughness variations on the adhesive performance of *L. caerulea* and *H. cinerea* studied here as well as of various tree frog species studied in previous research [34,43,50,52]. The adhesion performance of *L. caerulea* and *H. cinerea*, approximated by the falling angle $\alpha_\perp$, is approximately constant up to a roughness of 15 µm, showing that tree frogs are well able to adhere to substrates with a wide range of roughness. Also the adhesion $F_\perp$ and tenacity $\sigma_\perp$ barely differ on all tested substrates except the macrorough one. Such an insensitivity of adhesion towards substrate roughness is beneficial, as tree frogs encounter various roughness levels in their natural habitat, ranging from smooth to microrough leaves (e.g. $R_a \approx 0.5$–100 µm [55]) to macrorough tree bark. In the following, we discuss the adhesion performance of the toe pads for the different roughness levels, from smooth over micro- to macrorough substrates. As the friction data are largely confounded by the contact of belly and other body portions, we discuss these only where helpful.

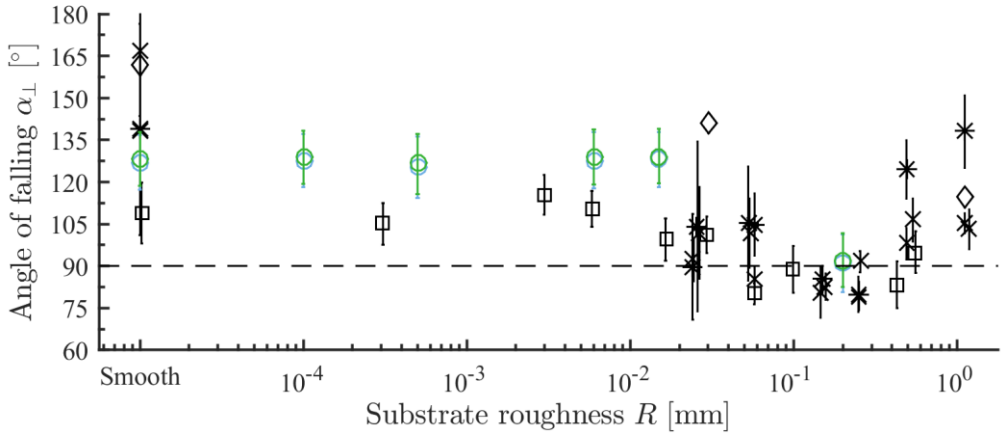

Figure 6. Adhesion performance of tree frogs as a function of (nominal) substrate roughness, indicated by the falling angles measured in this study (circles; means and 95% confidence intervals predicted from a linear mixed-effects model, *Litoria caerulea* [blue], *Hyla cinerea* [green]) and reported in literature (asterisks from Fig. 5 in [50], *Hyla microcephala*; crosses from Fig. 8a in [43], *Colostethus trinitatis*; diamonds from Fig. 3b in [52], *Rhacophorus pardalis*; squares from Fig. 1B in [34], *Litoria caerulea*). For smooth substrates, R = 10 nm is assumed. Falling angles below 90° (dashed line) indicate full adhesive failure. Due to only small interspecific differences, the blue and green circles are almost overlapping.

The falling angles of *L. caerulea* and *H. cinerea* measured on the smooth substrate fall within the range of 100–180° reported in literature (Figure 6). This large range arises from several causes. Most importantly, the attachment performance of tree frogs scales intra- and interspecifically with body size: As reported in this study and elsewhere [50,66,67], falling angles scale negatively with body mass. The correction for body mass in the linear mixed-effects model removes this size effect, resulting in $\alpha_{\perp} \approx 127.5°$. Whereas the superficial morphology of the adhesive pad does not seem to differ between the two species (see Figure SI.9; [51,52]), interspecific differences in animal behaviour, in the chemistry of the secreted mucus, or in the internal morphology of the toe pads [68] may explain the interspecific differences in attachment performance. Also, differences in substrate properties other than roughness should be considered. In this study, a hydrophilic epoxy resin with—compared to glass—relatively low free surface energy was used. We are not aware of extensive experimental studies on the effects of variations of free surface energy on tree frog attachment [69], and differences in free surface energy and hence in adhesion performance between the different studies (e.g. glass and aluminium oxide polishing paper in [34]) cannot be excluded.

On microrough substrates (i.e. 0.1 µm < R < 15 µm), the adhesion performance does not differ compared to the smooth substrate, as shown by the linear mixed-effects model for falling angles, and by the transformation of falling angles to adhesion forces or tenacities. Only for *H. cinerea*, tenacities are significantly higher on the 0.1 µm and the 15 µm substrate compared to the smooth one. These results are only partially in line with the findings of Crawford et al. [34], who described for single pads of *L. caerulea* significantly higher tenacities for R = 0.3–16 µm, if compared to a smooth substrate. Presumably, this disagreement between rotation platform experiments and single pad studies arises from differences in pad loading. Normal as well as shear loading have been shown to be important factors in determining the attachment performance of tree frog toe pads [26,70], which is discussed in more detail in Section 4.3.

In general, adhesion performance changes only little with an increasing substrate roughness from smooth to ca. 40 µm (Figure 6). Neither does adhesion performance increase abruptly with increasing roughness, as expected for biological attachment systems using mechanical interlocking (e.g. the claws of the beetles *Gastrophysa viridula* [44] and *Pachnoda marginata* [47], or of the may fly larva *Epeorus assimilis* [48]), nor does it drop suddenly, as hypothesised when the substrate asperities become too large to allow mechanical interlocking with the nano- to microscopic features of the ventral pad surface [53]. Importantly, the toe pads of tree frogs are very soft (with an effective elastic modulus of ca. 20–50 kPa; [41,71,72]), potentially allowing a close conformation to a rough substrate, an increase in the effective contact area, and as a result enhanced van der Waals forces (e.g. [73]). Therefore, one cannot exclude that at different roughness levels the effects of mechanical interlocking and other possibly involved attachment mechanisms cancel each other, leading to a constant attachment performance with increasing roughness. For further studies of the pad conformability, we suggest the visualisation of the pad-substrate contact for varying roughness levels. A detailed interpretation of the effects of variations in the complex phenomenon roughness [74] on tree frog attachment is challenging, also because of the presence of mucus in the contact area. Based on a discussion of the roughness parameters computed from the bearing area curves of the used substrates (see Section SI.2.1), one can conclude that the adhesion performance of tree frogs does not change despite a continuous increase in total roughness height S_{tot} up to ca. 4 µm and in reduced peak height S_{pk} up to almost 3 µm between the smooth and the 15 µm substrate. As asperities are a primary prerequisite for mechanical interlocking, this speaks against an appreciable contribution of mechanical interlocking to tree frog attachment.

A comparison with the attachment performance of other bioadhesive systems from various clades on rough substrates helps to further explore the fundamentals of tree frog attachment. For example, the hairy toe pads of insects (e.g. *G. viridula*, [44]*; Leptinotarsa decemlineata*,

374 [75]), arachnids (*Philodromus dispar*, [76]), and geckos (*Gekko gecko*, [77]) perform worse on
375 microrough substrates (typically in a range of 0.3–1.0 µm) than on smooth ones, which is gen-
376 erally explained by a loss of effective contact area for dry adhesion. Similar observations were
377 made for the smooth adhesive pads of insects (*Cydia pomonella*, [78]) and arachnids (*Ixodes*
378 *ricinus*, [79]). Such a decline in attachment performance is clearly not observed for tree frogs
379 in the microrough regime. This may be explained by the high pad conformability, which pre-
380 sumably facilitates a close pad-substrate contact and vdW force generation (Figure SI.10) on
381 microrough substrates, as proposed by [34]. Independence of the attachment performance on
382 roughness variations in between 0 µm and 12 µm has also been reported for the hairy adhesive
383 pads on the prey-capture apparatus of beetles in the genus *Stenus* [80]. The authors related this
384 independence partially to the small tip diameter (0.17–0.24 µm) of the hairy structures, which
385 may widen the range of substrate roughness which the pads can conform to. The nanopillars on
386 tree frogs' toe pads have a similar size (diameter ≈ 0.3 µm, [21]), possibly indicating a func-
387 tional analogy. Alternatively, the compensatory action of capillary adhesion may explain these
388 findings, as suggested by the increase in tree frog adhesion on rough substrates when adding
389 liquid [43,50,52].

390 On macrorough substrates (i.e. $R > 40$ µm), adhesion decreases gradually from $R \approx 40$ µm
391 to a local minimum at $R \approx 200$ µm, suggesting a gradually progressing failure of the involved
392 attachment mechanism(s) with increasing roughness. Such failure could be the cavitation of the
393 liquid meniscus and hence the loss of capillary adhesion [34,43,50]. Alternatively, a gradual
394 loss of effective contact area and of vdW forces with increasing roughness may lead to adhesive
395 failure, as aforementioned at lower roughness levels for the pads of lizards, insects, and arach-
396 nids. For $R > 200$ µm, adhesion seemingly increases again. This may indicate mechanical in-
397 terlocking of the whole toe pad with macroscopic surface asperities [43]. Here, the distal phal-
398 anx, which in many species is pointy (with a tip diameter of ca. 60 µm in *H. cinerea* [68]) and

399 extends distally into the subepidermal pad space [81], may act as ‘internal claw’. Also, Huber
400 et al. [77] suggested for geckos that individual attachment units (i.e. setae) can conform to the
401 tops or sides of macroscopic substrate asperities. A similar mechanism could apply to the indi-
402 vidual epidermal cells on tree frogs’ toe pads (Figure SI.10).

403 Further work is required for a full explanation of the attachment performance of tree frogs
404 on rough substrates. In order to test for the potential role of vdW forces, we suggest the direct
405 quantification of the conformability of tree frog toe pads to micro- to macrorough substrates.
406 Furthermore, a detailed analysis of the meniscus geometry for different roughness levels is
407 needed to illuminate the role of capillary adhesion in tree frog attachment on rough substrates.
408 Little is known about the substrates and roughness levels which tree frogs experience in their
409 natural habitats [39]. As increasingly emerging in the field of gecko adhesion [82,83], we pro-
410 pose ecomorphological analyses of tree frogs’ toe pads in order to explore correlations between
411 parameters of pad morphology (e.g. of the superficial epidermal cells [67]), ecology and natural
412 substrate properties, and attachment performance.

413 ## 4.2 Maximum attachment performance of tree frogs

414 Using whole-animal rotation platform experiments, we measured mean tenacities of approxi-
415 mately 2.5 mN mm^{-2} and a peak tenacity of 8.8 mN mm^{-2}. These values are considerably
416 higher than the tenacities of around 1 mN mm^{-2} measured in previous rotation platform studies
417 [25,26,51,66,67]. However, our results agree well with peak tenacities of up to ca. 8 mN mm^{-2}
418 that were recently reported for single pads adhering to a microrough substrate [34]. The devia-
419 tion in tenacity from earlier studies presumably relates to several factors. Most importantly, we
420 measured the instantaneous contact area before detachment of only the toe pads in contact,
421 which is smaller than the total surface area of all pads considered in previous studies. For ex-
422 ample, we found that tree frogs can generate sufficient adhesion with only two limbs in contact,
423 approximately doubling the tenacity compared to a situation where all limbs are in contact.

Moreover, the falling angle measured here exceeds the values reported in most other studies (Figure 6). This deviation may relate to the used setup, substrates, and the experimental animals. We specifically designed a stiff rotation platform to reduce vibrations, the induction of stress, and hence the chance of 'premature detachment' because of jumping of the animals. Moreover, we used frogs from a laboratory population that were accustomed to handling and the setup in pilot trials. Other studies [51,66,67] relied on wild-caught animals, which possibly are more susceptible towards stress during experimental handling.

Moreover, the frogs sometimes swing backwards upon detachment of the forelimbs (Figure 4), which results in inertial forces acting in addition to the static body weight on the pad-substrate interface. To estimate the magnitude of these inertial forces, the backwards swinging frog may be simplified as an oscillating pendulum. The maximum tension acting in the string of a pendulum is three times its static weight [84]. Assuming the swinging frog as pendulum, we estimate that the toe pads can withstand a maximum load of around 26 mN mm^{-2}, which lies close to the peak tenacity of 22 mN mm^{-2} measured by Endlein et al. [70]. Assuming free fall of the animals, inertial forces may be even higher, as indicated by peak forces of 130 mN (*Osteopilus septentrionalis*, [26]) and 1270 mN (estimated from landing kinematics in *Trachycephalus resinifictrix*, [85]) generated by single pads and limbs during dynamic events.

In order to determine the 'true' maximum attachment performance of tree frogs in whole-animal measurements, an accurate quantification of the inertial loads acting on the toes during dynamic events by a full inverse dynamics analysis is required. Moreover, rather than studying the average attachment performance—as done here and in previous work—we suggest for future studies a focus on an in-depth analysis of peak performance situations (e.g. the peak performance for each individual on each substrate), which was not possible here due to a too low sample number (n = 4). In combination with whole-animal studies, we suggest the execution of single pad force measurements under specified dynamic loading conditions, as done in [70].

Overall, the results of this study indicate that the attachment performance of tree frogs may be at least one order of magnitude higher than reported in earlier works. This makes tree frogs an interesting model system for the development of biomimetic high-performance adhesives in a wet environment. However, several questions remain unanswered: What is the real maximum attachment performance of tree frogs? Which mechanisms do explain the generation of the high attachment forces? Addressing these questions is relevant for the future design of biomimetic adhesives inspired by tree frog toe pads. For example, Drotlef et al. [13] measured for a tree-frog-inspired PDMS surface covered with hexagonal micropillars tenacities of around 2–4 mN mm^{-2}. Such technical adhesives may benefit significantly from a better understanding of the mechanisms determining the maximum attachment performance of tree frogs.

4.3 Problems and perspectives

In this study, we used the rotation platform approach, which allows the collection of relatively large data sets. Also, attachment can be studied for a relatively natural body posture, because the artificial fixation of body parts performed in single pad studies [33,34,70] is not required. However, rotation platform experiments also have drawbacks, which we discuss below.

Friction and adhesion are computed from the angles of falling and sliding (see equations 1 and 2), respectively. This approach allows a quick and easy quantification of whole-animal adhesion and friction. However, the two forces are inherently coupled due to the performed vector composition of the body weight. Hence, the normal load pulling the animal off the substrate (which equals adhesion at the moment of detachment) cannot be controlled independently of the parallel load dragging the frog along the substrate (which equals static friction at the onset of sliding; Figure 7), and vice versa. For example, sliding occurred at a range of angles, for which the normal load was compressive as well as tensile, and at angles just before falling parallel loads varied by approximately 50% of the body weight (Figure 7). In tree frogs, adhesion depends on the amount of the shear load before detachment [42,70], and—although to our

knowledge not substantiated by measurements—friction also depends on normal loading (e.g. in Coulomb friction [86] or in lubricated systems [87]). Therefore, the interdependency of normal and shear loading in rotation platform experiments presumably leads to an artificially increased variation of the measured forces.

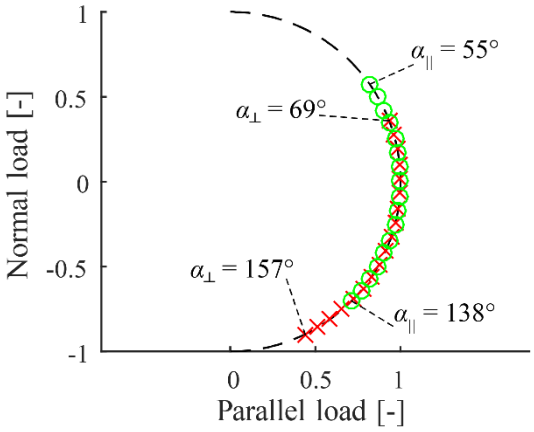

Figure 7. Interdependency of body-weight-normalised loads acting on a toe pad normal and parallel to the substrate in rotation platform experiments for the sliding ($\alpha_{||}$, green circles) and falling ($\alpha_{\perp}$, red crosses) angles measured in this study.

For evaluation of the adhesive whole-animal performance of tree frogs, we measured the instantaneous contact area of only the toe pads making contact with the substrate just before detachment. In previous works [26,50,66,67], it was assumed that the contact area is formed by the ventral surface areas of all toes of an individual, which presumably has led to an underestimation of the tenacity of tree frogs. Therefore, this study is an important step towards a more accurate quantification of the attachment performance, and an understanding of the fundamental attachment mechanisms of these animals. Such an understanding requires a detailed analysis of the fractions of the overall contact area, which are effective in the generation of wet and dry contact forces, respectively, and of the effective contact area on rough substrates. Such an analysis cannot be achieved with the FTIR technique used here. In future studies, optical methods (e.g. interference reflection microscopy [33,34]) or mechano-sensitive substrate coatings [88] could be used to measure the detailed characteristics of the contact area.

494 The quantification of the frictional performance of tree frog toe pads is confounded by
495 several factors. During sliding, large fractions of the contact area are formed by the belly and
496 other body portions, which has also been shown elsewhere [52,70]. As the belly and other body
497 portions can contribute considerably to the attachment of tree frogs [52], the rotation platform
498 is inappropriate for the analysis of the frictional performance of tree frogs' toe pads. Also, when
499 analysing sliding at angles of around 90°, it seemed that individuals of *H. cinerea* started sliding
500 with their frontlimbs but could still resist sliding with their hindlimbs. This observation indi-
501 cates that the assumption of equal loading of all toes is not fulfilled, as to be expected for the
502 required moment balance during steady attachment [68]. Such an unequal load distribution may
503 also occur at the angle of falling, reducing the effective measured adhesion. Differences in the
504 sliding of single toes may also explain the larger variation in sliding angles compared to the
505 measured falling angles. Lastly, it is difficult—if not impossible—to quantify the willingness
506 of a tree frog to attach to a substrate. We found a relatively large variation of the falling angles
507 per substrate and species, and of the number of successful trials per individual. In future rotation
508 platform experiments, such behavioural differences among individuals may be considered, for
509 example by including individual variability as random effect in the statistical model, as done in
510 this study.

511 Statistical models such as the linear mixed-effects model used here may help to cope with
512 the large variation in rotation platform studies. Temperature and relative air humidity should be
513 controlled to test for the effects of variations of these parameters on tree frog attachment. Com-
514 plementarily, single pad measurements with controlled shear loads in adhesion measurements
515 and vice versa, as in [42,70], will help to deepen the understanding of tree frog attachment.

516 ## 5 Conclusions

517 What is the maximum attachment performance of tree frogs on rough substrates? We address
518 this question by measuring the whole-animal attachment performance of the tree frog species

519 *Litoria caerulea* and *Hyla cinerea* on smooth, micro-, and macrorough substrates using a rota-
520 tion platform setup. The adhesive performance of the toe pads of tree frogs is insensitive to-
521 wards variations in substrate roughness up to a nominal roughness of ca. 40 µm. At higher
522 roughness levels up to $R \approx 200$ µm, adhesion decreases significantly compared to lower rough-
523 ness levels. The absence of a sudden increase in attachment performance when increasing the
524 roughness from smooth to microrough, and the absence of a stepwise decline in attachment
525 performance when further increasing the roughness negate a contribution of mechanical inter-
526 locking to tree frog attachment. Further work is required to elucidate if variations in substrate
527 roughness affect attachment force generation by capillary adhesion or by van der Waals inter-
528 actions (or by both mechanisms). Tree frogs were able to remain attached with only two limbs
529 in contact with an overhanging substrate. In agreement with recent studies, the tenacity of the
530 toe pads reaches peak values of up to 8.8 mN mm^{-2}, which is almost one order of magnitude
531 higher than reported previously. Inertial forces have to be considered in the quantification of
532 the maximum attachment performance, and we estimate that the maximum tenacity of tree
533 frogs' toe pads may be as much as 26 mN mm^{-2}.

534 ## Acknowledgements

535 This work is part of the research programme 'Secure and gentle grip of delicate biological tis-
536 sues' with project number 13353, which is financed by the Netherlands Organisation for Scien-
537 tific Research (NWO). We thank the following people for their valuable contributions. D. van
538 de Pol, S. van Woudenberg, S. Visser, and M. ter Veld from the CARUS research facility at
539 Wageningen University & Research (WUR), Wageningen, The Netherlands, set up and took
540 care of the populations of frogs used in this research. J. Belgraver and H. Meijer from the Tech-
541 nical Development Studio, WUR, assisted with designing and manufacturing the experimental
542 setup. A. Hagmayer and C. Voesenek, Experimental Zoology Group, WUR, helped with statis-
543 tical analysis and with MATLAB scripting, respectively. W.J.P. Barnes, Institute of Molecular,

Cell and Systems Biology, University of Glasgow, UK, provided helpful feedback on the experimental setup and animal housing. E.-J. Bakker, Biometris, WUR, provided advice on the statistical analysis, and R. Morssinkhof advised us on the housing of amphibians.

Author contributions

Conception of the study: JKAL, AR, JLvL; Development and testing of experimental setup: JKAL, RP, AR; Data collection: AR, JKAL; Data analysis: JKAL, AR; Data interpretation: JKAL, AR, JLvL; Drafting of the manuscript and figures: JKAL; Literature analysis: JKAL, SNG; Substrate preparation and characterisation methodology, and equipment: SNG, AK; Critical revision and approval: all authors.

References

[1] Peattie A M 2009 Functional demands of dynamic biological adhesion: an integrative approach *Journal of Comparative Physiology B* **179** 231–239
[2] Creton C and Gorb S N 2007 Sticky feet: From animals to materials *Materials Research Society Bulletin* **32** 466–472
[3] Favi P M, Sijia Y, Lenaghan S C, Xia L and Zhang M 2014 Inspiration from the natural world: from bio-adhesives to bio-inspired adhesives *Journal of Adhesion Science and Technology* **28** 290–319
[4] Gebeshuber I C 2007 Biotribology inspires new technologies *Nano Today* **2** 30–37
[5] Lepora N F, Verschure P and Prescott T J 2013 The state of the art in biomimetics *Bioinspiration & Biomimetics* **8** 1–11
[6] Byern J von and Grunwald I 2010 *Biological adhesive systems: From nature to technical and medical application* (Wien, New York: Springer)
[7] Smith A M 2016 *Biological adhesives* (Cham, Switzerland: Springer)
[8] Bogue R 2008 Biomimetic adhesives: a review of recent developments *Assembly Automation* **28** 282–288
[9] Flammang P and Santos R 2015 Biological adhesives: from biology to biomimetics *Interface Focus* **8** 1–3
[10] Li Y, Krahn J and Menon C 2013 Bioinspired dry adhesive materials and their application in robotics: A review *Journal of Bionic Engineering* **13** 181–199
[11] Barnes W J P 2007 Biomimetic solutions to sticky problems *Science* **318** 203–204
[12] Chen H, Zhang L, Zhang D, Zhang P and Han Z 2015 Bioinspired surface for surgical graspers based on the strong wet friction of tree frog toe pads *ACS Applied Materials & Interfaces* **7** 13987–13995
[13] Drotlef D-M, Stepien L, Kappl M, Barnes W J P, Butt H-J and del Campo A 2013 Insights into the adhesive mechanisms of tree frogs using artificial mimics *Advanced Functional Materials* **23** 1137–1146
[14] Jagota A and Hui C-Y 2011 Adhesion, friction, and compliance of bio-mimetic and bio-inspired structured interfaces *Materials Science and Engineering R* **72** 253–292

[15] Kamperman M, Kroner E, del Campo A, McMeeking R M and Arzt E 2010 Functional adhesive surfaces with ‘gecko‘ effect: The concept of contact splitting *Advanced Engineering Materials* **12** 335–348
[16] Autumn K, Liang Y A, Hsieh S T, Zesch W, Chan W P, Kenny T W, Fearing R and Full R J 2000 Adhesive force of a single gecko foot-hair *Nature* **405** 681–685
[17] Autumn K, Sitti M, Liang Y A, Peattie A M, Hansen W R, Sponberg S, Kenny T W, Fearing R, Israelachvili J N and Full R J 2002 Evidence for van der Waals adhesion in gecko setae *Proceedings of the National Academy of Sciences of the United States of America* **99** 12252–12256
[18] Filippov A E and Gorb S N 2015 Spatial model of the gecko foot hair: functional significance of highly specialized non-uniform geometry *Interface Focus* **5** 1–7
[19] Huber G, Gorb S N, Spolenak R and Arzt E 2005 Resolving the nanoscale adhesion of individual gecko spatulae by atomic force microscopy *Biology Letters* **1** 2–4
[20] Ernst V V 1973 The digital pads of the tree frog, *Hyla cinerea*. I. The epidermis *Tissue and Cell* **5** 83–96
[21] Scholz I, Barnes W J P, Smith J M and Baumgartner W 2009 Ultrastructure and physical properties of an adhesive surface, the toe pad epithelium of the tree frog, *Litoria caerulea* White *Journal of Experimental Biology* **212** 155–162
[22] Haslam I S, Roubos E W, Mangoni M L, Yoshizato K, Vaudry H, Kloepper J E, Pattwell D M, Maderson P F A and Paus R 2014 From frog integument to human skin: dermatological perspectives from frog skin biology *Biological Reviews* **89** 618–655
[23] Stebbins R C and Cohen N W 1995 *A natural history of amphibians* (Princeton, USA: Princeton University Press)
[24] Wells K D 2007 *The ecology & behaviour of amphibians* (Chicago, USA: The University of Chicago Press)
[25] Emerson S B and Diehl D 1980 Toe pad morphology and mechanisms of sticking in frogs *Biological Journal of the Linnean Society* **13** 199–216
[26] Hanna G and Barnes W J P 1991 Adhesion and detachment of the toe pads of tree frogs *Journal of Experimental Biology* **155** 103–125
[27] Nachtigall W 1974 *Biological Mechanisms of Attachment: The Comparative Morphology and Bioengineering of Organs for Linkage, Suction, and Adhesion* (Berlin, Heidelberg, New York: Springer Verlag)
[28] Schuberg A 1891 Über den Bau und die Funktion der Haftapparate des Laubfrosches *Arbeiten aus dem Zoologisch-Zootomischen Institut in Würzburg* **10** 57–119
[29] Siedlecki M 1909 Zur Kenntnis des javanischen Flugfrosches *Biologisches Centralblatt* **29** 704–715
[30] Wittich v. 1854 Der Mechanismus der Haftzehen von *Hyla arborea Archiv für Anatomie, Physiologie und Wissenschaftliche Medicin* 170–184
[31] Barnes W J P 2012 Adhesion in wet environments: Frogs *Encyclopedia of Nanotechnology* ed B Bhushan (Springer) pp 70–83
[32] Endlein T and Barnes W J P 2015 Wet adhesion in tree and torrent frogs *Encyclopedia of Nanotechnology* ed B Bhushan (Springer) pp 1–20
[33] Federle W, Barnes W J P, Baumgartner W, Drechsler P and Smith J M 2006 Wet but not slippery: boundary friction in tree frog adhesive toe pads *Journal of The Royal Society Interface* **3** 689–697
[34] Crawford N, Endlein T, Pham J T, Riehle M and Barnes W J P 2016 When the going gets rough – studying the effect of surface roughness on the adhesive abilities of tree frogs *Beilstein Journal of Nanotechnology* **7** 2116–2131
[35] Green D M 1981 Adhesion and the toe-pads of treefrogs *Copeia* **1981** 790–796

[36] Komnick H and Stockem W 1969 Oberfläche und Verankerung des Stratum corneum an mechanisch stark beanspruchten Körperstellen beim Grasfrosch *Cytobiologie: Zeitschrift für experimentelle Zellfoschung* **1** 1–16
[37] Emerson S B 1991 The ecomorphology of Bornean tree frogs (family Rhacophoridae) *Zoological Journal of the Linnean Society* **101** 337–357
[38] Green D M and Simon M P 1986 Digital microstructure in ecologically diverse sympatric microhylid frogs, genera *Cophixalus* and *Sphenophryne* (Amphibia : Anura), from Papua New Guinea *Australian Journal of Zoology* **34** 135–45
[39] Moen D S, Irschick D J and Wiens J J 2013 Evolutionary conservatism and convergence both lead to striking similarity in ecology, morphology and performance across continents in frogs *Proceedings of the Royal Society B: Biological Sciences* **280** 1–9
[40] Sustaita D, Pouydebat E, Manzano A, Abdala V, Hertel F and Herrel A 2013 Getting a grip on tetrapod grasping: form, function, and evolution *Biological Reviews* **88** 380–405
[41] Barnes W J P, Goodwyn P J P, Nokhbatolfoghahai M and Gorb S N 2011 Elastic modulus of tree frog adhesive toe pads *Journal of Comparative Physiology A* **197** 969–978
[42] Barnes W J P, Pearman J and Platter J 2008 Application of peeling theory to tree frog adhesion, a biological system with biomimetic implications *E-Newsletters for Science and Technology, Published by European Academy of Sciences (EAS)* **1** 1–2
[43] Barnes W J P, Smith J, Oines C and Mundl R 2002 Bionics and wet grip *Tire Technology International* 56–60
[44] Bullock J M R and Federle W 2011 The effect of surface roughness on claw and adhesive hair performance in the dock beetle *Gastrophysa viridula Insect Science* **18** 298–304
[45] Klittich M R, Wilson M C, Bernard C, Rodrigo R M, Keith A J, Niewiarowski P H and Dhinojwala A 2017 Influence of substrate modulus on gecko adhesion *Scientific Reports* **7** 1–10
[46] Stark A Y, Badge I, Wucinich N A, Sullivan T W, Niewiarowski P H and Dhinojwala A 2013 Surface wettability plays a significant role in gecko adhesion underwater *Proceedings of the National Academy of Sciences of the United States of America* **110** 6340–6345
[47] Dai Z, Gorb S N and Schwarz U 2002 Roughness-dependent friction force of the tarsal claw system in the beetle *Pachnoda marginata* (Coleoptera, Scarabaeidae) *Journal of Experimental Biology* **205** 2479–2488
[48] Ditsche-Kuru P, Barthlott W and Koop J H E 2012 At which surface roughness do claws cling? Investigations with larvae of the running water mayfly *Epeorus assimilis* (Heptageniidae, Ephemeroptera) *Zoology* **115** 379–388
[49] Vakis A I, Yastrebov V A, Scheibert J, Minfray C, Nicola L, Dini D, Almqvist A, Paggi M, Lee S, Limbert G, Molinari J F, Anciaux G, Aghababaei R, Restrepo S E, Papangelo A, Cammarata A, Nicolini P, Putignano C, Carbone G, Ciavarella M, Stupkiewicz S, Lengiewicz J, Costagliola G, Bosia F, Guarino R, Pugno N M and Müser M H 2018 Modeling and simulation in tribology across scales: An overview *Tribology International* 1–84
[50] Barnes W J P 1999 Tree frogs and tire technology *Tire Technology International* 42–47
[51] Barnes W J P, Oines C and Smith J M 2006 Whole animal measurements of shear and adhesive forces in adult tree frogs: insights into underlying mechanisms of adhesion obtained from studying the effects of size and scale *Journal of Comparative Physiology A* **192** 1179–1191
[52] Endlein T, Barnes W J P, Samuel D S, Crawford N A, Biaw A B and Grafe U 2013 Sticking under wet conditions: The remarkable attachment abilities of the torrent frog, *Staurois guttatus PLoS ONE* **8** 1–12

[53] Ernst V V 1973 The digital pads of the tree frog, *Hyla cinerea*. II. The mucous glands *Tissue and Cell* **5** 97–104
[54] Linnenbach M 1985 Zum Feinbau der Haftscheiben von *Hyla cinerea* (Schneider, 1799) (Salientia: Hylidae) *Salamandra* **21** 81–85
[55] Koch K, Bhushan B and Barthlott W 2008 Diversity of structure, morphology and wetting of plant surfaces *Soft Matter* **4** 1943–1963
[56] Brehm A E 1892 *Brehms Tierleben: allgemeine Kunde des Tierreichs* vol 7, ed E Pechuel-Loesche (Leipzig, Wien: Bibliographisches Institut)
[57] Gadow H 1909 *Amphibia and Reptiles* (London, UK: MacMillan and Co.)
[58] Gorb S N 2007 Visualisation of native surfaces by two-step molding *Miscroscopy Today* **15** 44–47
[59] Koch K, Schulte A J, Fischer A, Gorb S N and Barthlott W 2008 A fast, precise and low-cost replication technique for nano- and high-aspect-ratio structures *Bioinspiration & Biomimetics* **3** 1–10
[60] Kaelble D H 1970 Dispersion-polar surface tension properties of organic solids *The Journal of Adhesion* **2** 66–81
[61] Owens D K and Wendt R C 1969 Estimation of the surface free energy of polymers *Journal of Applied Polymer Science* **13** 1741–1747
[62] Rabel W 1971 Einige Aspekte der Benetzungstheorie und ihre Anwendung auf die Untersuchung und Veränderung der Oberflächeneigenschaften von Polymeren *Farbe und Lack* **77** 997–1005
[63] Hill I D ., Dong B, Barnes W J P, Ji A and Endlein T 2018 The biomechanics of tree frogs climbing curved surfaces: a gripping problem *Journal of Experimental Biology* **221** 1–10
[64] Burnham K P and Anderson D R 2002 *Model Selection and Multimodel Inference: A Practical Information-Theoretic Approach* (New York: Springer)
[65] Endlein T, Ji A, Samuel D, Yao N, Wang Z, Barnes W J P, Federle W, Kappl M and Dai Z 2012 Sticking like sticky tape: tree frogs use friction forces to enhance attachment on overhanging surfaces *Journal of The Royal Society Interface* **10** 1–11
[66] Smith J M, Barnes W J P, Downie J R and Ruxton G D 2006 Adhesion and allometry from metamorphosis to maturation in hylid tree frogs: a sticky problem *Journal of Zoology* **270** 372–383
[67] Smith J M, Barnes W J P, Downie J R and Ruxton G D 2006 Structural correlates of increased adhesive efficiency with adult size in the toe pads of hylid tree frogs *Journal of Comparative Physiology A* **192** 1193–1204
[68] Langowski J K A, Schipper H, Blij A, Berg F T van den, Gussekloo S W S and Leeuwen J L van 2018 Force-transmitting structures in the digital pads of the tree frog *Hyla cinerea*: a functional interpretation *Journal of Anatomy* **233** 478–495
[69] Langowski J K A, Dodou D, Kamperman M and Leeuwen J L van 2018 Tree frog attachment: mechanisms, challenges, and perspectives *Frontiers in Zoology* **15:**32 1–21
[70] Endlein T, Ji A, Yuan S, Hill I, Wang H, Barnes W J P, Dai Z and Sitti M 2017 The use of clamping grips and friction pads by tree frogs for climbing curved surfaces *Proceedings of the Royal Society B: Biological Sciences* **284** 1–9
[71] Barnes W J P, Baum M, Peisker H and Gorb S N 2013 Comparative cryo-SEM and AFM studies of hylid and rhacophorid tree frog toe pads *Journal of Morphology* **274** 1384–1396
[72] Kappl M, Kaveh F and Barnes W J P 2016 Nanoscale friction and adhesion of tree frog toe pads *Bioinspiration & Biomimetics* **11**
[73] Purtov J, Gorb E V, Steinhart M and Gorb S N 2013 Measuring of the hardly measurable: adhesion properties of anti-adhesive surfaces *Applied Physics A* **111** 183–189

[74] Persson B N J, Albohr O, Tartaglino U, Volokitin A I and Tosatti E 2005 On the nature of surface roughness with application to contact mechanics, sealing, rubber friction and adhesion *Journal of Physics: Condensed Matter* **17** 1–62
[75] Voigt D, Schuppert J M, Dattinger S and Gorb S N 2008 Sexual dimorphism in the attachment ability of the Colorado potato beetle *Leptinotarsa decemlineata* (Coleoptera: Chrysomelidae) to rough substrates *Journal of Insect Physiology* **54** 765–776
[76] Wolff J O and Gorb S N 2012 Surface roughness effects on attachment ability of the spider *Philodromus dispar* (Araneae, Philodromidae) *Journal of Experimental Biology* **215** 179–184
[77] Huber G, Gorb S N, Hosoda N, Spolenak R and Arzt E 2007 Influence of surface roughness on gecko adhesion *Acta Biomaterialia* **3** 607–610
[78] Al Bitar L, Voigt D, Zebitz C P W and Gorb S N 2010 Attachment ability of the codling moth *Cydia pomonella* L. to rough substrates *Journal of Insect Physiology* **56** 1966–1972
[79] Voigt D and Gorb S 2017 Functional morphology of tarsal adhesive pads and attachment ability in ticks *Ixodes ricinus* (Arachnida, Acari, Ixodidae) *Journal of Experimental Biology* **220**
[80] Koerner L, Gorb S N and Betz O 2012 Adhesive performance of the stick-capture apparatus of rove beetles of the genus *Stenus* (Coleoptera, Staphylinidae) toward various surfaces *Journal of Insect Physiology* **58** 155–163
[81] Manzano A S, Fabrezi M and Vences M 2007 Intercalary elements, treefrogs, and the early differentiation of a complex system in the Neobatrachia *The Anatomical Record* **290** 1551–1567
[82] Collins C E, Russell A P and Higham T E 2015 Subdigital adhesive pad morphology varies in relation to structural habitat use in the Namib day gecko *Functional Ecology* **29** 66–77
[83] Elstrott J and Irschick D J 2004 Evolutionary correlations among morphology, habitat use and clinging performance in Caribbean Anolis lizards *Biological Journal of the Linnean Society* **83** 389–398
[84] Bel é ndez A, Francés J, Ortuño M, Gallego S and Bernabeu J G 2010 Higher accurate approximate solutions for the simple pendulum in terms of elementary functions *Europena Journal of Physics* **31** 65–70
[85] Bijma N N, Gorb S N and Kleinteich T 2016 Landing on branches in the frog *Trachycephalus resinifictrix* (Anura: Hylidae) *Journal of Comparative Physiology A* **202** 267–276
[86] Israelachvili J N 2011 *Intermolecular and surface forces* (Amsterdam: Elsevier)
[87] Pitenis A A, Urueña J M, Schulze K D, Nixon R M, Dunn A C, Krick B A, Sawyer W G and Angelini T E 2014 Polymer fluctuation lubrication in hydrogel gemini interfaces *Soft Matter* **10** 8955–8962
[88] Neubauer J W, Xue L, Erath J, Drotlef D-M, del Campo A and Fery A 2016 Monitoring the Contact Stress Distribution of Gecko-Inspired Adhesives Using Mechano-Sensitive Surface Coatings *ACS Applied Materials & Interfaces* **8** 17870–17877